# Quasi-Biennial and Quasi-Decadal Variations in Snow Accumulation over Northern Eurasia and Their Connections to the Atlantic and Pacific Oceans

HENGCHUN YE

*Department of Geography and Urban Analysis, California State University, Los Angeles, California*

(Manuscript received 21 August 2000, in final form 11 June 2001)

ABSTRACT

Spatial and temporal characteristics of winter snow depth variation over northern Eurasia and their connections to sea surface temperatures (SSTs) and associated atmospheric circulation anomalies, surface air temperatures, and precipitation are examined by using 60 yr (1936–95) of station data records. This study found that snow depth variation over the region east of the Caspian Sea and west of China, explaining 10.1% of total snow depth variance, has a quasi-biennial variability of about 2.5 yr. The snow depth variation over central European Russia and western-central Siberia, explaining 8.1% of the total snow depth variance, has a quasi-decadal variability of about 11.8 yr. The snow depth variation over the northern Ural Mountains, explaining 7.5% of the total snow depth variance has, variability of about 8 and 14 yr.

The quasi-biennial snow depth variation is associated with SSTs over the northern North Pacific and tropical western Atlantic extending into the Gulf of Mexico. The associated atmospheric circulation pattern of Eurasia 1 (EU-1) and the Pacific–North American (PNA) pattern determine the surface air temperature conditions and thus snow depth at the biennial timescale. The quasi-decadal snow variation is associated with a well-known SST anomaly pattern over the Atlantic, having opposite SST variations in alternating latitudinal belts, and SSTs over the tropical Pacific Ocean. The associated atmospheric North Atlantic oscillation (NAO) and the circulation anomaly over central Siberia affect both surface air temperature and precipitation and thus snow depth anomaly on this quasi-decadal timescale. The results provide observational evidence of possible causes for snow depth variability over high-latitude regions.

## 1. Introduction

Snow accumulation is the result of complex interactions between precipitation and air temperature. Atmospheric circulation affects both precipitation and temperature conditions and hence snow accumulations. The atmosphere also closely interacts with SSTs over certain regions of the oceans (e.g., Delworth and Stouffer 1993; Graham 1994; Lau 1997; Wallace et al. 1990). As a result, the variability of snow accumulation in certain regions is probably teleconnected to SST anomalies.

Eurasian snow, covering the largest land area of the Northern Hemisphere, influences climate worldwide. It directly affects land surface temperature and thus atmospheric circulation through the albedo effect and soil moisture conditioning after melting (e.g., Barnett et al. 1989; Watanabe and Nitta 1998; Yasunari et al. 1991). It also modifies the Arctic and nearby oceans through the feedback of freshwater runoff, sea ice distribution, salinity, and thermohaline circulation (e.g., Aagaard and Carmack 1989; Hibler and Zhang 1995; Mysak et al. 1990). The spatial variability of Eurasian snow coverage has been studied since the availability of advanced very high resolution radiometer (AVHRR) observations via satellite (e.g., Clark et al. 1999; Frei and Robinson 1999; Robinson et al. 1993). Due to the short length of available snow coverage data, temporal variability other than trends has not been examined in these studies.

Modeling studies have shown that snow depth rather than snow spatial coverage has a more significant impact on global climate in subsequent seasons by altering the hydrological cycle and hence the surface energy budget (e.g., Barnett et al. 1989; Yasunari et al. 1991). Thus, snow depth is an important aspect of snow accumulation in addition to spatial coverage. Since the publication of the first CD-ROM containing station snow depth records over the former Soviet Union by the National Snow and Ice Data Center (NSIDC), snow depth trend and spatial and temporal variability have been studied (Ye et al. 1998; Ye 2000). However, potential causes for variability have not been examined extensively other than connections to Atlantic sea surface temperature (SST) anomalies (Ye 2000). In this study, the author uses snow depth records updated to 1995, the second version of the CD recently published by NSIDC, to examine con-

*Corresponding author address:* Dr. Hengchun Ye, Department of Geography and Urban Analysis, California State University, Los Angeles, 5151 State University Dr., Los Angeles, CA 90032-8222.
E-mail: hengchun.ye@calstatela.edu

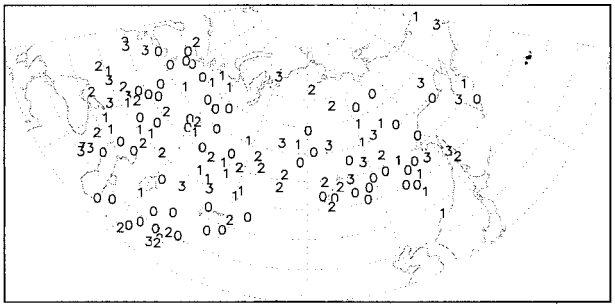

FIG. 1. Snow station locations and number of missing winters during the 60-yr study period from 1936 to 1995.

nections between the regional variability of snow depth and SSTs over both the Atlantic and Pacific Oceans. In addition, the snow depth trend up to 1995 is reevaluated and associated surface air temperature, precipitation, and atmospheric circulation anomalies are examined.

## 2. Data

### *a. Snow depth and trends*

Monthly snow depth for January, February, and March is derived from the Historical Soviet Daily Snow Depth CD-ROM Version 2.0 available from the NSIDC. The original daily snow data were calculated by averaging the readings from three measuring rods in a meteorological enclosure surrounding each station. Each reading was rounded to the nearest centimeter. A more complete and better quality control routine than the earlier version (Version 1) has been developed and applied to this dataset.

The original daily records include 184 stations covering the time period from 1881 to 1995 with many missing values in early years. Since winter snow depth has a high temporal continuity over regions, the winter monthly mean snow depth is averaged from daily records if there are at least eight days of observation for that month. Analysis of the error generated by an 8-day monthly snow depth average (Dr. R. Brown 2001, personal communication) revealed that this is only important where the mean monthly snow depth is less than 10 cm. More than 99% of the monthly snow depth values used in the study meet or exceed this threshold condition. Then, each missing month is interpolated from the month before and the month after if they are available. The winter seasonal mean snow depth is the average of the three monthly means of January, February, and March. As a result, 137 stations covering 60 yr from 1936 to 1995 having no more than 3 missing winters or a maximum of 5% missing values are selected for the study (Fig. 1). In average conditions, the significant correlation exists among stations (at a 90% significance level) within about 500 km over European Russia, about 320 km over western Siberia, about 270 km over central Siberia, and about 450 km over eastern Siberia. Considering the large spatial covariability of snow depth, these stations have a reasonably good spatial coverage in most areas of the study region.

The station data are then interpolated into grid points of 5° latitude by 5° longitude for each winter using Shepard's local-search interpolation on a spherical surface (Willmott et al. 1985). Stations that have missing values are not used in the interpolation for that particular winter. In Shepard's interpolation, the initial searching radian is determined by the average station distribution density, and the number of stations used for interpolation for each grid point is averaged at 7 (minimum 4 and maximum 10). A few grid points located on the edges of the study region that are too far away from stations to have reliable values are considered to be missing and a few grids located on water are also removed. A total of 154 grid points that have no missing values for the study time period are retained for further analyses (Fig. 2).

The mean snow depth for the 60-yr study period is displayed in Fig. 3. The highest snow depth (over 70 cm) is found over northern-central Siberia and another high snow depth center is located over the northern Ural Mountains. The latter is probably associated with orographic precipitation. Also, since most stations are biased to lower elevation, the snow depth data shown may be lower than actual values over mountain ranges. Low snow depth of less than 10 cm is found over southern regions.

To reexamine the snow depth trend for this study time period, a linear least square regression is developed for

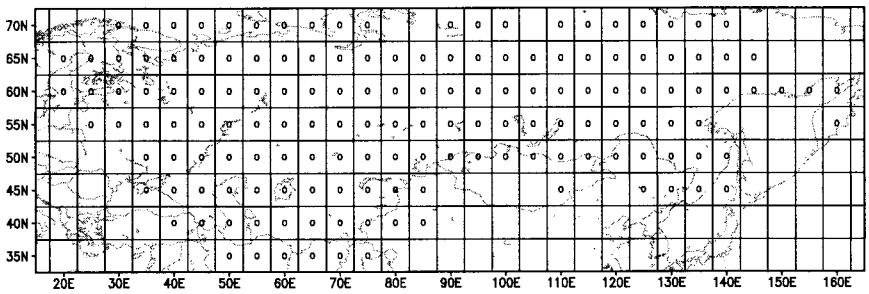


FIG. 2. Snow gridpoint distributions. The grid points marked by "o" represent no missing values for the study time period and are used in subsequent analyses.

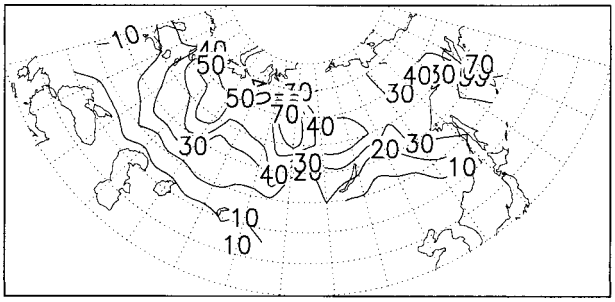

FIG. 3. Mean winter (Jan–Feb–Mar) snow depth (cm) from 1936 to 1995.

each grid point. The slope of the regression line for each grid point indicating the annual rate of change is plotted in Fig. 4a and expressed as % change per decade in Fig. 4b. Significant increasing trends in snow depth of 0.2–0.6 cm $yr^{-1}$ (5%–10% $decade^{-1}$) are observed over the northern Ural Mountains. These localized trends are slightly higher than the latitudinal average of 4.7% between 60° and 70°N for the time period of 1936–83 (Ye et al. 1998) and are consistent with winter precipitation trends of 6%–9% over the same locations and during a similar time period (Ye 2001).

The trend component for each grid point is removed from the original snow depth if the trend is statistically significant at a 95% confidence level. Then the detrended snow depth at each grid point is standardized before statistical analyses.

### b. Sea surface temperature

Sea surface temperature data are taken from the gridded monthly Global Sea-Ice and SST dataset (GISST, version 2.3b) compiled and quality controlled by the Hadley Centre for Climate Prediction and Research, Met Office. This dataset has a resolution of 1° latitude by 1° longitude and covers 1871 to the present (Folland and Parker 1995; Parker et al. 1995). Four different reconstruction methods were used to construct this SST dataset for the four different time periods of 1871–1902, 1903–48, 1949–81, and 1982 to the present as summarized by Hurrell and Trenberth (1999).

Although the SSTs from GISST for the most recent period after 1981 are not of as high a quality as those of the reynolds reconstruction of the Comprehensive Ocean–Atmosphere Data Set (COADS). (Hurrell and Trenberth 1999), a recent study by Ye (2001) suggests that teleconnections to northern-central Eurasian precipitation are not sensitive to the use of these two different sets of SST data. Thus, the GISST dataset is used due to its longer period of coverage. Grid points over both the Atlantic and Pacific Oceans between 20°S and 70°N are selected where SSTs of reasonably good quality are found (Hurrell and Trenberth 1999). The SSTs are detrended and standardized using the same methods as those applied to snow depth grid points.

### c. Surface air temperatures, precipitation, and 700-mb geopotential heights

Surface air temperatures at 184 stations over the study region during 1936–90 are selected (Fig. 5a). These monthly air temperature data are extracted from a large air temperature file consisting of all stations north of 40°N, originally compiled and quality checked at the National Prediction Center. Precipitation data at 261 stations extracted from the former Soviet Union Monthly Precipitation Archive, available from NSIDC are selected for this study (Fig. 5b). This precipitation dataset has been quality controlled and corrections have been made to justify for observation time and rain gauge changes, as well as wetting losses (Groisman et al. 1991). The time period covered is 1936–93.

Atmospheric circulation anomalies are represented by 700-mb geopotential heights from reanalysis products of the National Centers for Environmental Prediction (NCEP). The geopotential height data from this reanalysis are heavily influenced by observations and are considered to have a reasonably good quality of temporal continuity due to the consistency of treatment methods (Kalnay et al. 1996).

The mean winter temperatures, precipitation, and

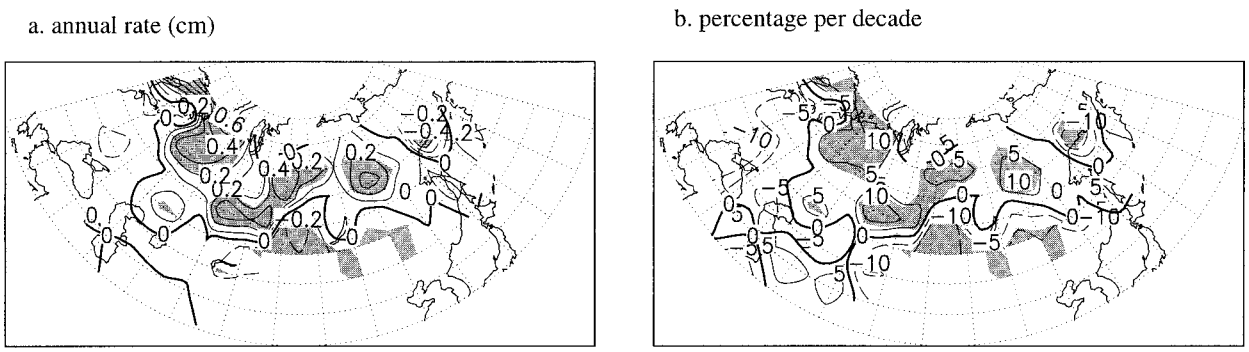


FIG. 4. Winter snow depth trend for the study period of 1936–95. (a) Annual rate of change (in cm), (b) percentage of change $decade^{-1}$. Shading represents statistically significant trends at a 95% confidence level.

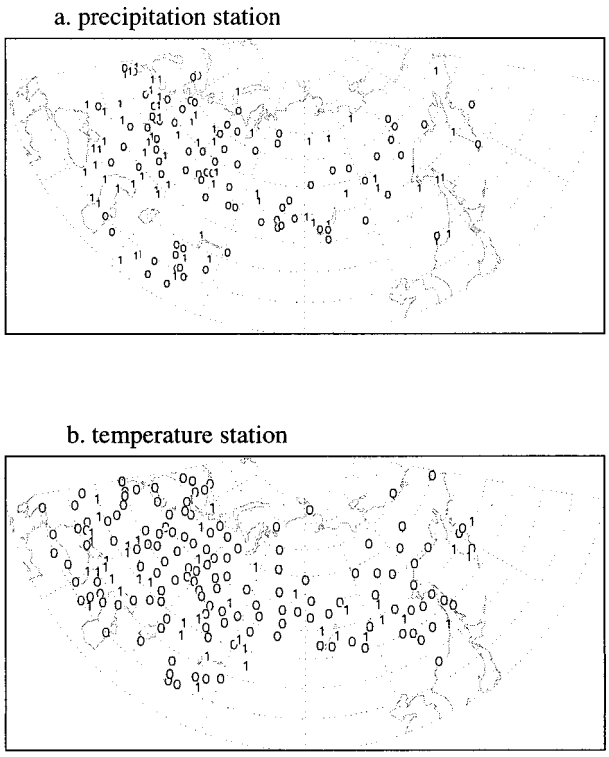


FIG. 5. Stations distributions for (a) precipitation during 1936–93. (b) Surface air temperature during 1936–90.

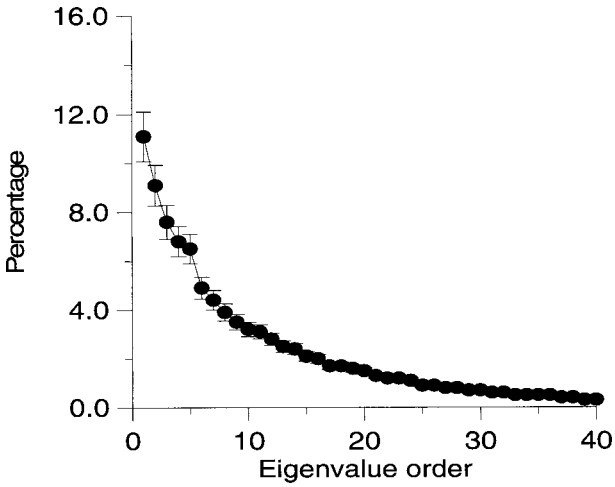


FIG. 6. The eigenvalue plot from (percentage of snow depth variation explained) PCA. Error bars are 95% confidence intervals based on North et al.'s (1982) formulation.

700-mb heights are the average of three monthly mean values of January, February, and March to be consistent with the snow depth data described above.

## 3. Methodology

Rotated principal component analysis (RPCA) is applied to the detrended grid points of snow depth to define major spatial variation patterns. Singular spectrum analysis (SSA) is applied to the time series of each retained major spatial variation pattern to reveal quasi-periodical variation characteristics. Cross-correlation maps displaying the correlation coefficients between SSTs of oceans and the time series of each snow depth variation pattern are produced to reveal the geographical regions over oceans where statistically significant correlations are present. In delineating statistically significant grids, the ''equivalent sample size'' used is estimated based on the autocorrelation coefficients (first order) in the time series of both snow depth and the grid points of SSTs (von Storch and Zwiers 1999). The composite departure maps showing differences between the highest positive and lowest negative phases of revealed oscillations in SSTs, air temperatures, precipitation, and 700-mb geopotential heights are produced to reveal the amplitudes of the associated quasi-periodical variations and connections among these different fields. The statistically significant areas of the composite maps are determined by a *t* test (95% confidence level for one-tail or 90% confidence level for two-tails) to determine whether the magnitude of departures between the highest-positive and lowest-negative phases is statistically significantly different.

Principal component analysis (PCA) is an effective way to reduce data dimension while retaining much of the variability inherent in the original data. The application of rotation after major variation patterns are retained is designed to produce physically meaningful and robust spatial patterns (Richman 1986).

SSA is a powerful tool for time series analysis that can identify intermittent oscillation spells in short noise time series. Mathematically, it is similar to PCA but reveals temporal variation patterns of a single time series using a predefined window length (Vautard et al. 1992; Plaut and Vautard 1994; Elsner and Tsonis 1996). SSA produces eigenvalues that are sorted in descending order. Two adjacent eigenvalues form a pair if they are nearly equal and together they potentially represent an oscillation component. The significance test for the oscillation pair against red noise is based on Allen and Smith's (1996) formulation of 10 000 Monte Carlo simulations of surrogate time series having the same mean, standard deviation, and the first-order autocorrelation of the original time series. If an eigenvalue from SSA is larger than the 97.5 percentile of those from simulations, then this eigenvalue is considered to explain more variance than a random red noise, and thus is considered to be significant at a 95% confidence level (Allen and Smith 1996).

The time evolution of each identified oscillation component is extracted from the original time series to produce a reconstructed oscillation component (Plaut and Vautard 1994; Vautard et al. 1992). These oscillation components are also correlated to SSTs (and 700-mb heights) to show the relative significance of telecon-

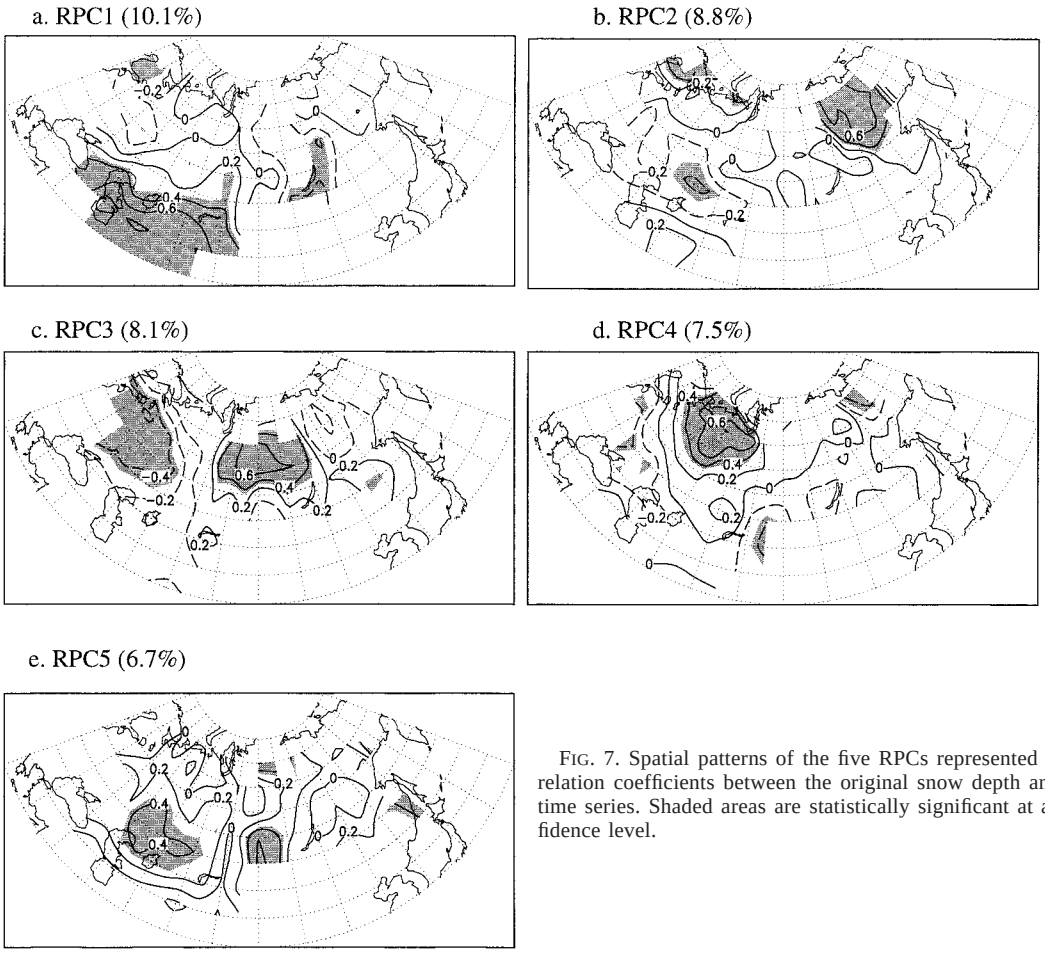


FIG. 7. Spatial patterns of the five RPCs represented by the correlation coefficients between the original snow depth and the RPC time series. Shaded areas are statistically significant at a 99% confidence level.

nections at the specified oscillation timescale versus those at an interannual timescale.

## 4. Results

### *a. Snow depth variability*

Five major snow depth variation patterns from PCA are retained for rotation. The selections are based on the significant break between the fifth and the sixth eigenvalue (Fig. 6). These 5 PCs together explain 41.2% of the total snow depth variation after trends have been removed.

Varimax rotation is performed on these five retained PCs. The resulting spatial patterns represented by the correlation coefficients between the grid points of snow depth and the corresponding rotated PC time series are illustrated in Fig. 7. The first rotated PC (RPC1; 10.1%) describes snow depth variation over the southwestern part of the study region, an area around the Caspian Sea and west of China. The second PC (RPC2; 8.8%) represents snow depth variation over the East Siberian Upland. The third PC (RPC3; 8.1%) has two significant opposing variation centers, one over central European Russia and the other over western-central Siberia. The fourth PC (RPC4; 7.5%) describes snow depth variation over the northwestern part of the study region, covering areas around the northern Ural Mountains. The fifth PC (RPC5; 6.7%) illustrates snow depth variation over southwestern Siberia and a few other small areas.

The time series of these 5 RPCs are shown in Fig. 8. In addition, moving averages are also overlaid to reveal low-frequency variation patterns that are evident in RPC3, RPC4, and RPC5.

SSA is applied to each of the five RPCs. In revealing temporal variability, any RPC that has an oscillation timescale longer than 20 yr is not emphasized in this study due to the relatively short data length (60 yr). As a result, three RPCs are found to have significant oscillation characteristics with timescales shorter than 20 yr. The identified oscillation components are at timescales of about 2.5 yr for RPC1, 11.8 yr for RPC3, and 8 and 14 yr for RPC4. These oscillations explain about 25.1%, 23.5%, and 19.2% of the variance of the corresponding RPC time series.

The eigenvalues and the estimated 97.5 percentiles of red noises from Monte Carlo simulations based on

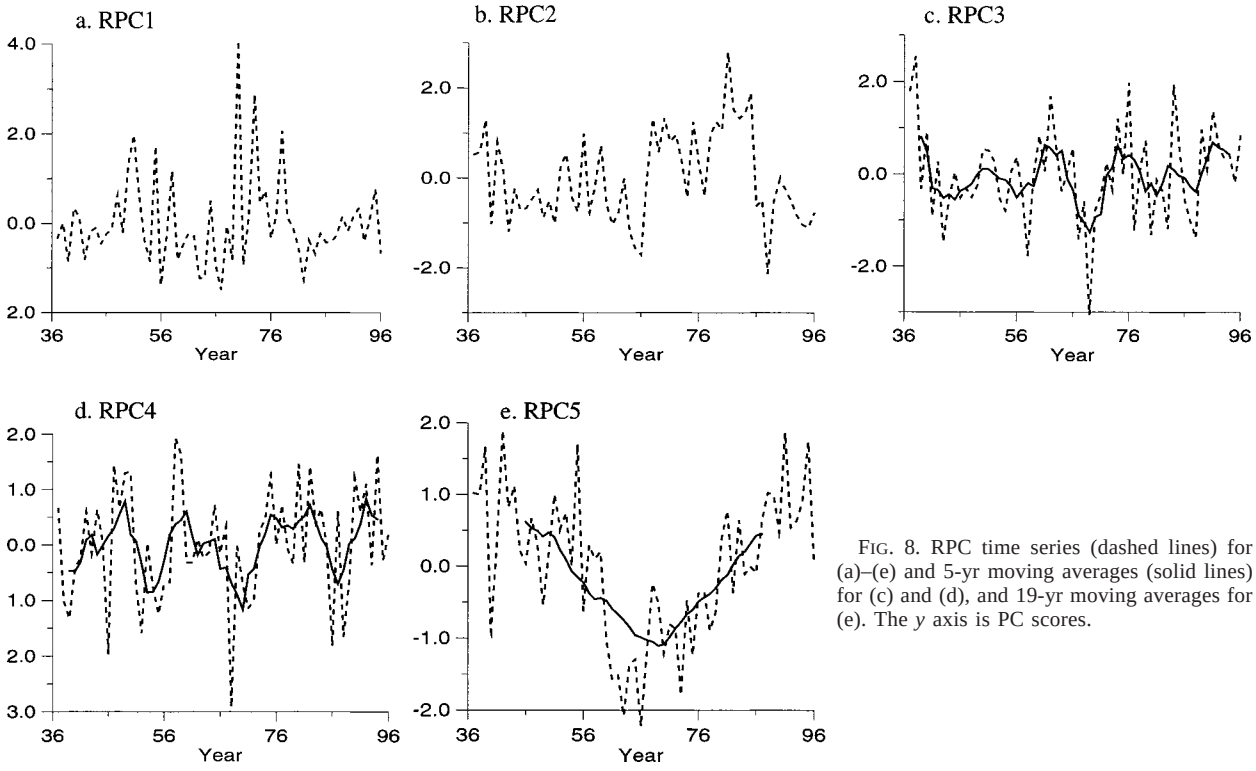


FIG. 8. RPC time series (dashed lines) for (a)–(e) and 5-yr moving averages (solid lines) for (c) and (d), and 19-yr moving averages for (e). The *y* axis is PC scores.

the formulation of Allen and Smith (1996) are plotted in Fig. 9. For RPC1, the first four eigenvalues are statistically significant above red noises (Fig. 9a), but only the second and third eigenvalues form an oscillation pair representing an oscillation at a timescale of about 2.5 yr. The first two eigenvalues from RPC2 are above the red noises and form an oscillation pair representing an oscillation at a timescale of about 11.8 yr (Fig. 9b). So are the first two eigenvalues of RPC4, which have two timescales, at about 8.3 and 14.3 yr (Fig. 9c).

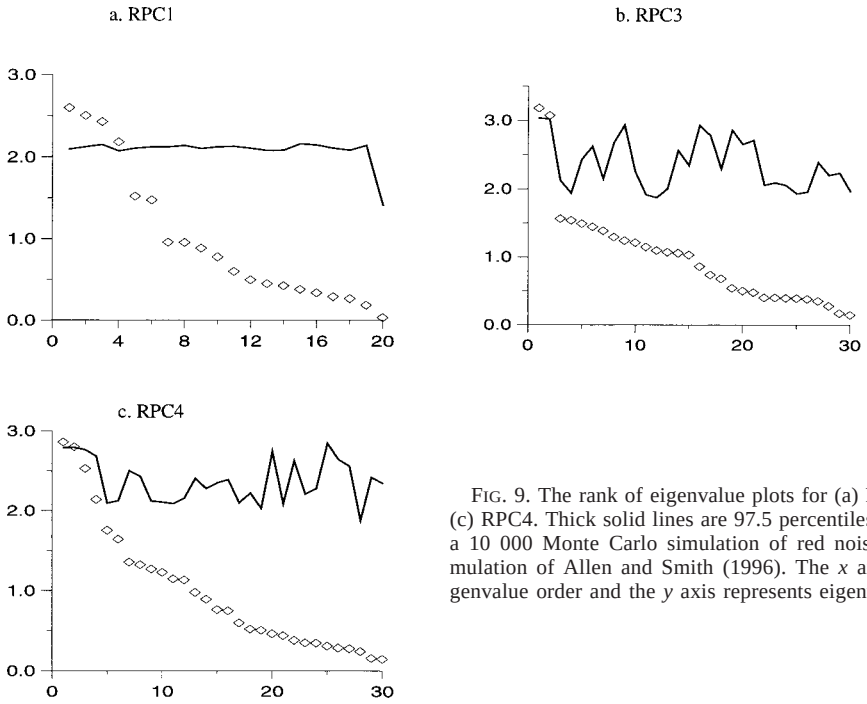


FIG. 9. The rank of eigenvalue plots for (a) RPC1, (b) RPC3, and (c) RPC4. Thick solid lines are 97.5 percentiles of eigenvalues from a 10 000 Monte Carlo simulation of red noises based on the formulation of Allen and Smith (1996). The *x* axis represents the eigenvalue order and the *y* axis represents eigenvalues.

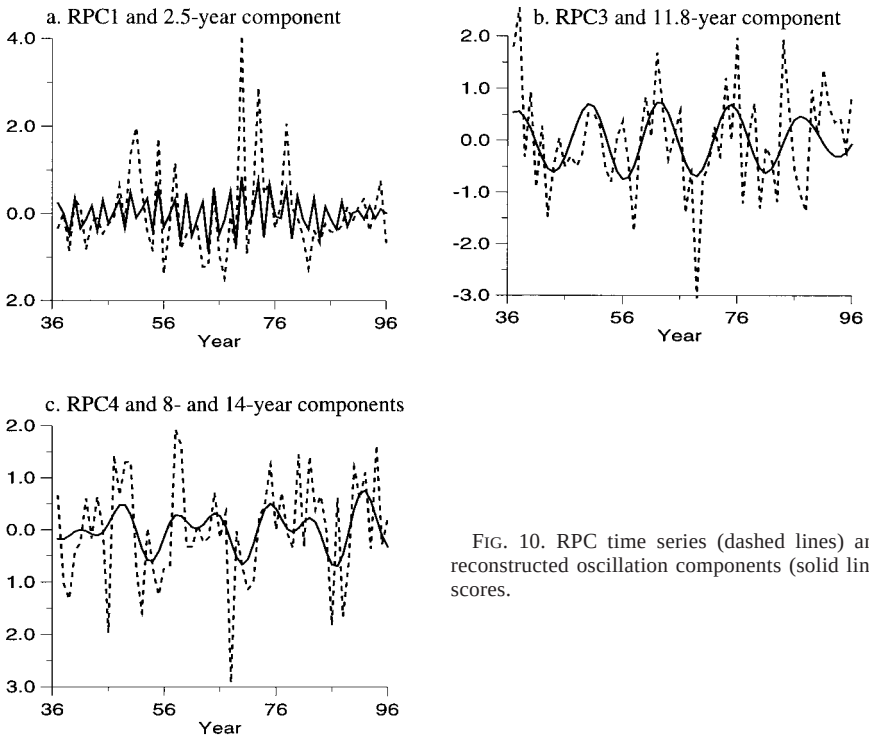


FIG. 10. RPC time series (dashed lines) and the corresponding reconstructed oscillation components (solid lines). The *y* axis is PC scores.

The reconstructed oscillation components along with the three time series of RPCs are plotted in Fig. 10 for visual examination and comparison with moving average lines in Fig. 8. The figure clearly shows that the reconstructed oscillation components are generally consistent with moving average lines.

### *b. Correlation with SSTs*

The correlation coefficients between grid points of SSTs over the oceans and each time series of RPCs and the reconstructed oscillation components are calculated. Only those RPCs that have statistically significant correlations to oceans are presented and retained for further analyses. RPC1 is positively correlated to SSTs over the central North Pacific and negatively correlated with those over the eastern North Pacific (west coast of North America) and the northern North Atlantic (Fig. 11a). When the correlation is done for the 2.5-yr reconstructed oscillation component, the significant correlation area is found in the southwestern Atlantic extending into the Gulf of Mexico while the general correlation coefficients pattern over the Pacific is similar to those of RPC1 (Fig. 11b).

RPC3 is correlated to SSTs mostly over the Atlantic Ocean (Fig. 12a) while its 11.8-yr oscillation component also has significant correlations to SSTs over the tropical Pacific Ocean (Fig. 12b). In addition, the alternating zonal correlation coefficients pattern over the Atlantic is better defined and correlation coefficients are higher in some latitudes in Fig. 12b. When correlation is calculated for the time series of the 5-yr moving average of RPC3, the coefficient pattern more closely resembles that of the reconstructed oscillation component than that of the original RPC3 (Fig. 12c). This suggests that the connection between snow depth over central European Russia and western-central Siberia and SSTs is more significant at a low-frequency mode of quasi-decadal timescale than at an interannual one.

The SST correlation coefficients pattern associated with quasi-decadal snow depth variation resembles the major SST pattern over the Atlantic Ocean that is associated with the North Atlantic oscillation (NAO) and the western Atlantic oscillation (Deser and Blackmon 1995; Lau and Nath 1994; Livezey and Smith 1999; Peng and Mysak 1993; Wallace et al. 1990; Xie and Tanimoto 1998). This connection is consistent with an earlier study using 48 yr of snow depth data and 40 yr of Atlantic SSTs (Ye 2000).

### *c. Composite departures*

To further reveal the amplitude of these oscillations and teleconnections, the composite departures of snow depth and SSTs between the positive and negative phases of the oscillation are calculated. In addition, the composites for surface air temperatures, precipitation, and atmospheric circulation are also produced to reveal potential contributors to snow depth variability.

For the 2.5-yr oscillation, there are 24 positive and 23 negative peak phases for the 60-yr period of snow depth data. The average snow depth for these positive

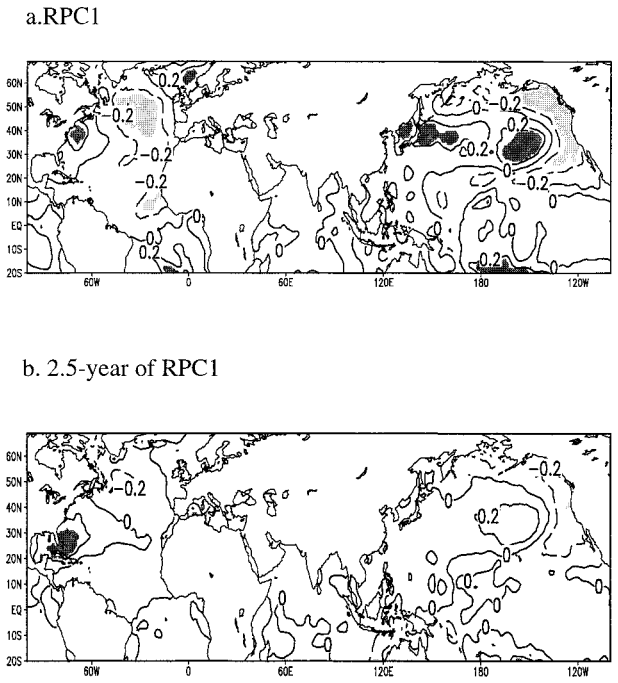


FIG. 11. Correlation coefficients between grid points of SSTs and RPC1 (a) and 2.5-yr oscillation component of RPC1 (b). Shaded areas are statistically significant at a 95% confidence level.

and negative phase years are averaged from original station snow depth records. Although the difference in snow depth over the southwestern study region is only about 1–2 cm (not shown), it is about 40%–100% of the mean snow accumulation of the region (Fig. 13a). This region is a transition zone between snow cover to the north and snow free to the south and is very sensitive to climate variation (Clark et al. 1999; Frei and Robinson 1999).

The composite map of surface air temperature shows a negative departure of about 1.5°C (Fig. 13b) while the precipitation does not have any significant departures over the region (Fig. 13c). This suggests that the higher snow depth years are associated with lower surface air temperature and are not related to the precipitation amount for the region east of the Caspian Sea and west of China.

The SST departure pattern resembles the map of correlation with the 2.5-yr oscillation component shown in Fig. 11b. Amplitude of about 0.2°C over the central North Pacific and 0.4°C over the western tropical Atlantic are found to be associated with this quasi-biennial oscillation. The latter's center is statistically significant at a 95% confidence level for a one-tail *t* test (Fig. 13d).

The 700-mb departure map shows three significant anomaly centers: the northern Pacific, European Russia, and central Siberia (Fig. 13e). These anomalies suggest an amplified wave pattern over northeastern Eurasia with a ridge over European Russia and a trough over central Siberia, favoring cold air sliding down to the area east of the Caspian Sea and west of China. The anomaly centers also correspond well to cross-correlation maps between RPC1 (and the 2.5-yr component) and 700-mb geopotential heights (not shown). The two Eurasian anomaly centers resemble the Eurasia Pattern 1 (EU-1; Barnston and Livizey 1987) and the northern Pacific anomaly coincides with one center of the Pacific–North America (PNA) pattern. These findings confirm a study by Clark et al. (1999) that found that the EU-1 pattern is the major atmospheric mechanism affecting winter snow coverage in the same region. Clark

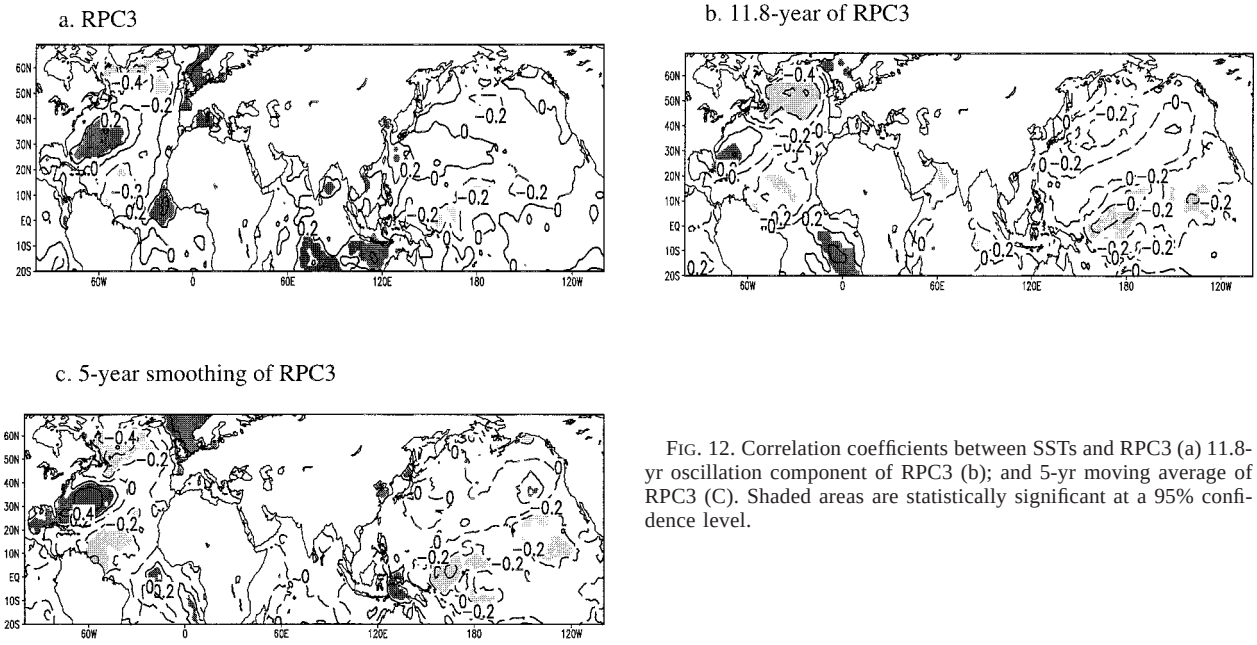


FIG. 12. Correlation coefficients between SSTs and RPC3 (a) 11.8-yr oscillation component of RPC3 (b); and 5-yr moving average of RPC3 (C). Shaded areas are statistically significant at a 95% confidence level.

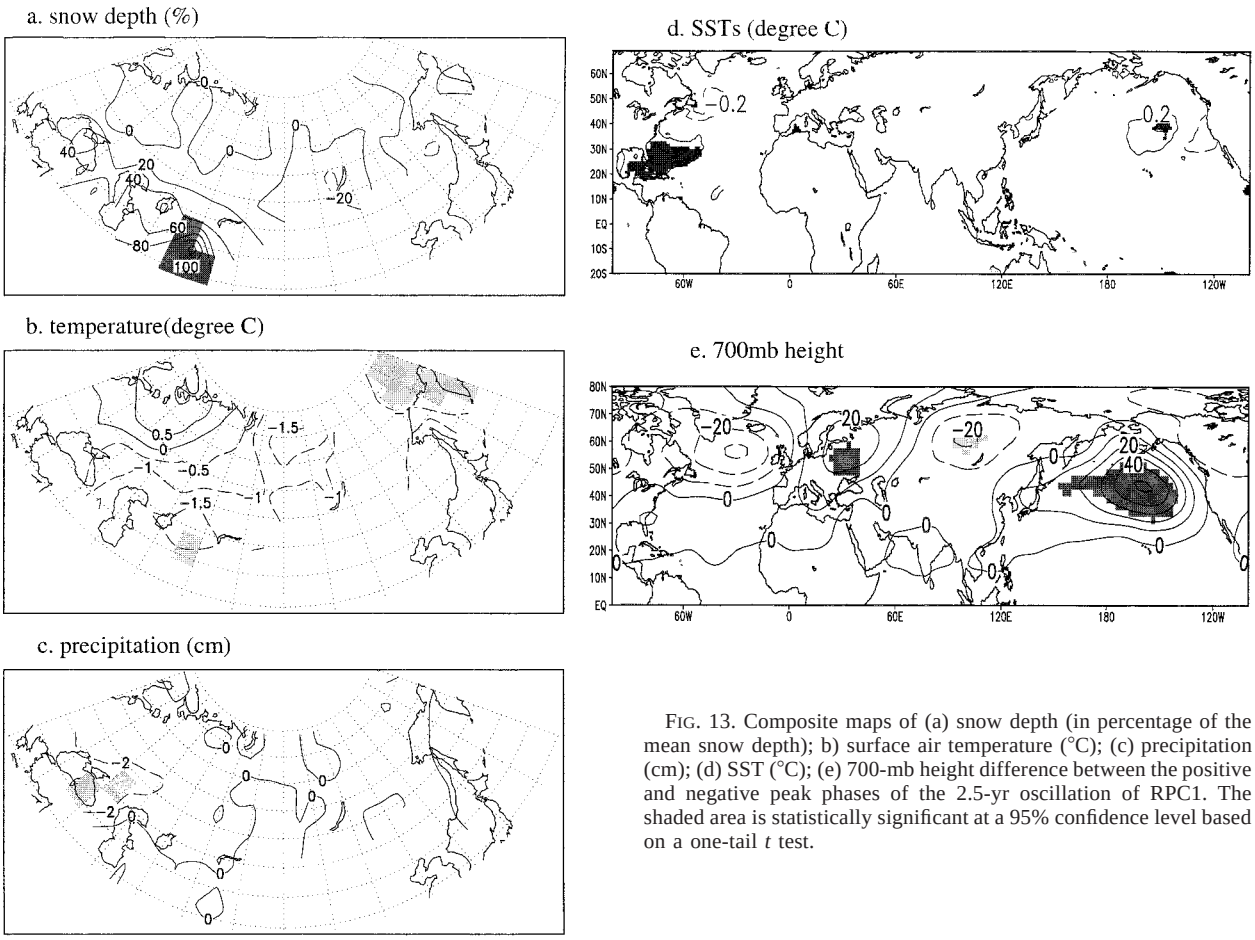


FIG. 13. Composite maps of (a) snow depth (in percentage of the mean snow depth); b) surface air temperature (°C); (c) precipitation (cm); (d) SST (°C); (e) 700-mb height difference between the positive and negative peak phases of the 2.5-yr oscillation of RPC1. The shaded area is statistically significant at a 95% confidence level based on a one-tail *t* test.

et al. (1999) suggested that during negative EU-1 phases, the snow cover area is larger than normal, which is likely due to lower temperatures over the region. This current study confirms the suspected lower surface air temperatures and higher snow depth under the negative EU-1 phases and vice versa. In conclusion, snow depth over the southwestern study region (an area east of the Caspian Sea and west of China) is dependent on surface air temperature conditions and is negatively correlated with the EU-1 and the PNA at a quasi-biennial timescale. The SST anomaly pattern is likely to interact with the PNA over the North Pacific and subsequently affect circulation downstream over Eurasia.

Five positive and negative peak phases are identified from the reconstructed 11.8-yr oscillation time series for the 60 yr of the study time period. Amplitudes of 5–10 cm in snow depth are found over European Russia and over western-central Siberia (not shown). These 5–10-cm departures account for about 40%–60% of the mean snow depth over these regions (Fig. 14a).

The composite map of air temperature shows north–south opposite departures: large positive temperature departures (up to 2.5°C) in northern European Russia and negative departures of about −1°C on the southern edge of European Russia (Fig. 14b). This suggests that during positive phases of quasi-decadal snow depth variation, the surface air temperature is higher over northern and lower over southern European Russia. Precipitation departures have a negative center of 2–4 cm over central European Russia and positive values of 2 cm over central Siberia as shown on the composite map (Fig. 14c). The negative precipitation center overlaps the southern negative snow depth center. It is likely that the large positive temperature departures reduce snow depth over northern European Russia and thus the northward location of the negative snow departure center in relation to the precipitation departures. Thus, snow depth over European Russia is determined both by precipitation and temperature anomalies over the region.

Composite departures of SSTs between the positive and negative peak phases of the 11.8-yr oscillation component are shown in Fig. 14d. To increase the sample size for the statistical *t* test, the two highest-positive and lowest-negative years instead of one for each cycle are used in the composites of SSTs associated with the 11.8-yr oscillation. So, 8 and 9 yr corresponding to the two consecutive highest-positive and lowest-negative phases are used in the SST composite associated with this var-

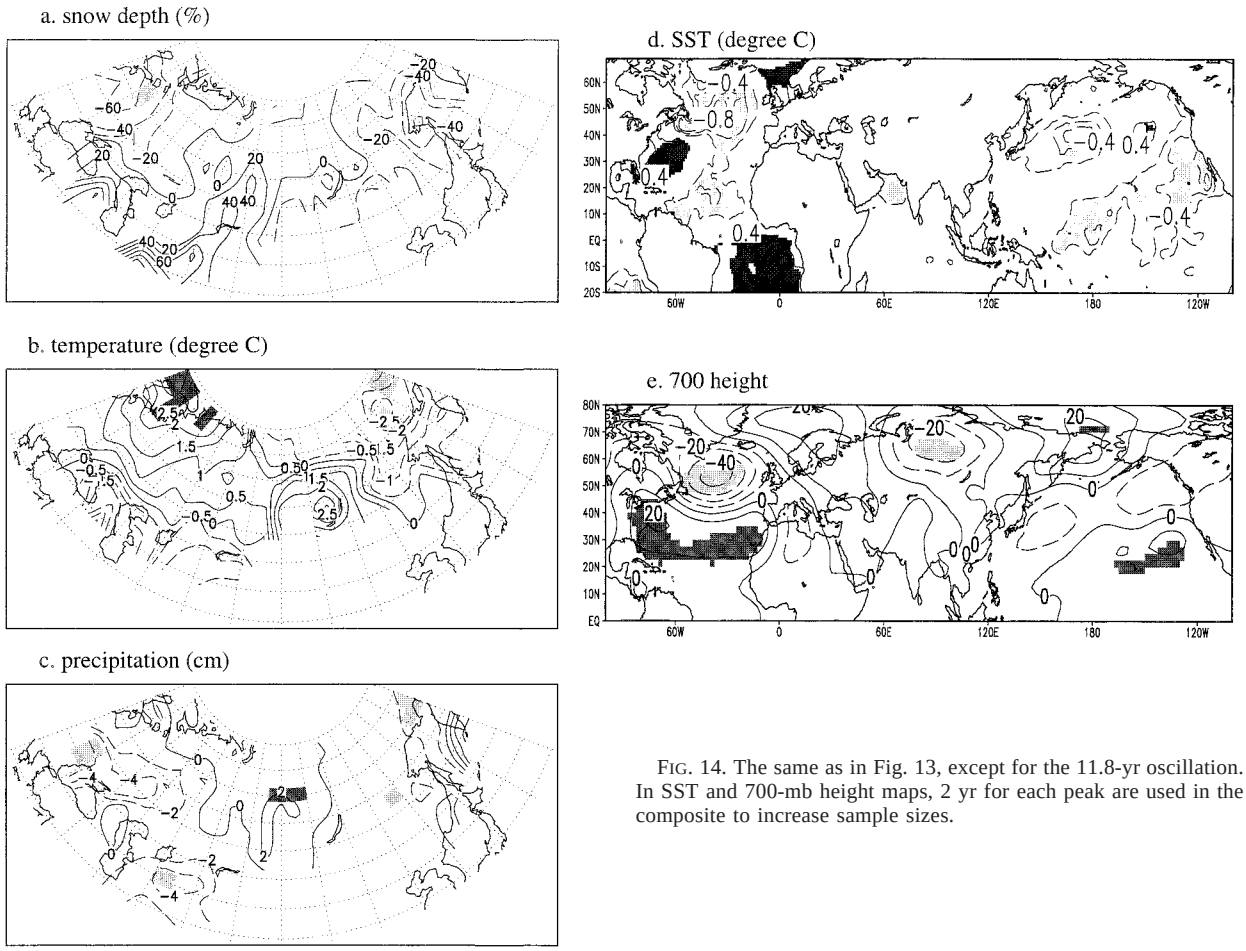


FIG. 14. The same as in Fig. 13, except for the 11.8-yr oscillation. In SST and 700-mb height maps, 2 yr for each peak are used in the composite to increase sample sizes.

iability. The magnitude of SST anomalies ranges from 0.2° to 0.8°C and most areas are statistically significant at a 95% confidence level for a one-tail *t* test.

The associated 700-mb height departures (sample sizes of 7 and 8 yr for the positive and negative phases, respectively) are over Greenland, the southern North Atlantic, central Siberia, and the eastern tropical Pacific (Fig. 14e). The first two centers resemble the NAO (Barnston and Livezey 1987). The NAO-associated atmospheric circulation anomaly over the eastern tropical Pacific Ocean off the coast of California has also been described by Rogers (1984). This Pacific circulation anomaly center obviously corresponds to the quasi-decadal variation of tropical Pacific SSTs that covariates with those over the Atlantic Ocean.

In positive (negative) NAO phases, cyclones are likely to track northward (southward) bringing increased (decreased) temperatures and decreased (increased) precipitation to Europe (Clark et al. 1999; Hurrell 1995; Rogers 1997; Serreze et al. 1997). This is consistent with the finding of this snow depth study that positive (negative) NAO phases result in increased (decreased) air temperatures observed over northern European Russia and decreased (increased) precipitation over central European Russia and thus below (above) normal snow accumulation over European Russia. During these positive NAO phases, central Siberia is likely responsible for the increased precipitation and thus snow depth over western Siberia. And this connection has quasi-decadal timescale characteristics of about 11.8 yr.

## 5. Summary

Spatial and temporal variation characteristics of winter snow accumulation over northern-central Eurasia during 1936–95 are examined. In addition to positive trends over much of the central and northern study region and negative trends over some southern areas, three major variation modes are found. These are quasi-biennial of about 2.5 yr over a large area east of the Caspian Sea and west of China, quasi-decadal of about 11.8 yr over central European Russia and western-central Siberia, and about 7 and 14 yr around the northern Ural Mountains.

The quasi-biennial variation of snow depth is associated with SST anomalies over the central North Pacific and tropical western Atlantic extending into the Gulf of Mexico. The atmospheric circulation patterns that

bridge this connection are the EU-1 and the PNA that determine surface air temperature over the region. Surface air temperature rather than precipitation is the major factor determining snow depth over the area east of the Caspian Sea and west of China.

The quasi-decadal variation of snow depth over central European Russia and western-central Siberia is associated with a well-known SST anomaly pattern over the Atlantic, having opposite variations in alternating latitudinal belts. This Atlantic SST pattern is also associated with SSTs over the tropical Pacific Ocean at a quasi-decadal timescale. The NAO determines both air temperature and precipitation anomalies over northern-central Eurasia. Under a positive (negative) phase of the NAO, air temperature is warmer (colder) over northern and colder (warmer) over southern European Russia and precipitation is less (more) over central European Russia and more (less) over western-central Siberia, thus resulting in lower (higher) snow depth over central European Russia and higher (lower) snow depth over western-central Siberia.

The quasi-biennial variation in the PNA has been revealed in other studies (e.g., Barnston et al. 1991; Trenberth and Shin 1984). The quasi-biennial covariation of surface air temperatures found over the United States and Europe extending to areas east of the Caspian Sea (Mann and Park 1994) suggests the presence of covariation between the EU-1 and the PNA at this particular timescale.

The SST and atmospheric variation patterns over the Pacific associated with quasi-biennial variability resemble those associated with interdecadal variation of the Pacific (Deser and Blackmon 1995; Trenberth and Hurrell 1994; Zhang et al. 1997) instead of those that are concentrated in tropical regions where a larger amplitude of quasi-biennial variability is to be expected (e.g., Barnett 1991; Cariolle et al. 1993). This may suggest that tropical and extratropical biennial variations do not occur in phases and thus the tropical SSTs do not show significant correlations here. On the other hand, SST variations over both the eastern tropical and the extratropical Pacific seem to be associated with El Niño. Atmospheric circulation bridges the link between tropical and extratropical SST variations (Lau 1997). In other words, all these different timescale variations is SSTs over different regions of the Pacific are manifestations of different aspects of El Niño (Barnett 1991; Trenberth 1976; Zhang et al. 1997). The biennial variation that is revealed in this study is suspected to be one aspect of El Niño's effects on air temperature and snow depth in a region east of the Caspian Sea through the concurrent atmospheric PNA and EU-1 circulation patterns.

The quasi-decadal SST and atmospheric circulation patterns are consistent with those revealed in a study of precipitation variation over European Russia (Ye 2001). In addition, a similar teleconnection to the Atlantic Ocean has also been revealed in an earlier snow depth study for the time period of 1936–83 (Ye 2000). The close geographical region and timescales of connections from these independent studies using different historical records/data length further verify the strong signals of this teleconnection. Combined with results from European climate variation studies (Hurrell 1995; Hurrell and von Loon 1997; Rogers 1997), it seems that the furthest influence of the Atlantic Ocean (including the NAO) on the precipitation and snow depth of northern Eurasia is on western-central Siberia with the most direct influence on the west side of the Ural Mountains.

*Acknowledgments.* This work is supported by the NSF Geography and Regional Science Program and Climate Dynamics Program. The author thanks Drs. Cort J. Willmott, Scott M. Robeson, Michael J. Janis, and Andrew J. Grundstein for valuable discussions on Shepard's interpolation method. The author also appreciates Dr. Pasha Ya. Groisman's updated precipitation dataset and his comments as well as Argyl B. Houser for editing the final draft of this paper. Appreciation is extended to the data providers: the National Snow and Ice Data Center for snow records, the Hadley Centre for Climate Prediction and Research, Met Office for sea surface temperatures, NCEP for 700-mb geopotential heights, and Drs. Jon Eischeid and Tingjun Zhang for station temperature records. Ross D. Brown and an anonymous reviewer's valuable comments have improved the quality of this paper significantly.

## REFERENCES

Aagaard, K., and E. C. Carmack, 1989: The role of sea ice and other fresh water in the Arctic circulation. *J. Geophys. Res.,* **94** (C10), 14 485–14 498.

Allen, M. R., and L. A. Smith, 1996: Monte Carlo SSA: Detecting irregular oscillations in the presence of colored noise. *J. Climate,* **9,** 3373–3404.

Barnett, T. P., 1991: The interaction of multiple time scales in the tropical climate system. *J. Climate,* **4,** 269–285.

——, L. Dümenil, U. Schlese, E. Roeckner, and M. Latif, 1989: The effect of Eurasian snow cover on regional and global climate variations. *J. Atmos. Sci.,* **46,** 661–685.

Barnston, A. G., and R. E. Livezey, 1987: Classification, seasonality and persistence of low-frequency atmospheric circulation patterns. *Mon. Wea. Rev.,* **115,** 1083–1126.

——, ——, and M. S. Halpert, 1991: Modulation of Southern Oscillation–Northern Hemisphere mid-winter climate relationships by the QBO. *J. Climate,* **4,** 203–217.

Cariolle, D., M. Amidei, M. Déqué, J.-F. Mahfouf, P. Simon, and H. Teyssédre, 1993: A quasi-biennial oscillation signal in general circulation model simulations. *Science,* **261,** 1313–1316.

Clark, M. P., M. C. Sierreze, and D. A. Robinson, 1999: Atmospheric controls on Eurasian snow extent. *Int. J. Climatol.,* **19,** 27–40.

Delworth, T. L., and R. J. Stouffer, 1993: Interdecadal variations of the thermohaline circulation in a coupled ocean–atmosphere model. *J. Climate,* **6,** 1993–2011.

Deser, C., and M. L. Blackmon, 1995: On the relationship between tropical and North Pacific sea surface temperature variations. *J. Climate,* **8,** 1677–1680.

Elsner, J. B., and A. A. Tsonis, 1996: *Singular Spectrum Analysis: A New Tool in Time Series Analysis.* Plenum Press, 164 pp.

Folland, C. K., and D. E. Parker, 1995: Correction of instrumental biases in historical sea surface temperature data. *Quart. J. Roy. Meteor. Soc.,* **121,** 319–367.

Frei, A., and D. A. Robinson, 1999: Northern Hemisphere snow extent: Regional variability 1972–1994. *Int. J. Climatol.,* **19,** 1535–1560.

Graham, N. E., 1994: Decadal-scale climate variability in the tropical and North Pacific during the 1970s and 1980s: Observations and model results. *Climate Dyn.,* **10,** 135–162.

Groisman, P. Ya., V. V. Koknaeva, T. A. Belodylova, and T. R. Karl, 1991: Overcoming biases of precipitation measurement: A history of the USSR experience. *Bull. Amer. Meteor. Soc.,* **72,** 1725–1733.

Hibler, W. D., III, and J. Zhang, 1995: On the effect of sea-ice dynamics on oceanic thermohaline circulation. *Ann. Glaciol.,* **21,** 361–368.

Hurrell, J. W., 1995: Decadal trends in the North Atlantic oscillation: Regional temperatures and precipitation. *Science,* **269,** 676–679.

——, and H. von Loon, 1997: Decadal variations in climate associated with the North Atlantic oscillation. *Climatic Change,* **36,** 301–326.

——, and K. E. Trenberth, 1999: Global sea surface temperature analyses: Multiple problems and their implications for climate analysis, modeling, and reanalysis. *Bull. Amer. Meteor. Soc.,* **80,** 2661–2678.

Kalnay, E., and Coauthors, 1996: The NCEP/NCAR 40-Year Reanalysis Project. *Bull. Amer. Meteor. Soc.,* **77,** 437–471.

Lau, N.-C., 1997: Interactions between global SST anomalies and the midlatitude atmospheric circulation. *Bull. Amer. Meteor. Soc.,* **78,** 21–33.

——, and M. J. Nath, 1994: A modeling study of the relative roles of tropical and extratropical SST anomalies in the variability of the global atmosphere–ocean system. *J. Climate,* **7,** 1184–1207.

Livezey, R. E., and T. M. Smith, 1999: Covariability of aspects of North American climate with global sea surface temperatures on interannual to interdecadal timescales. *J. Climate,* **12,** 289–302.

Mann, M. E., and J. Park, 1994: Global-scale modes of surface temperature variability on interannual to century timescales. *J. Geophys. Res.,* **99,** 25 819–25 833.

Mysak, L. A., D. K. Manak, and R. F. Marsden, 1990: Sea-ice anomalies observed in the Greenland and Labrador Seas during 1901–1984 and their relation to an interdecadal Arctic climate cycle. -*Climate Dyn.,* **5,** 111–133.

North, G. R., L. B. Thomas, and R. F. Cahalan, 1982: Sampling errors in the estimation of empirical orthogonal functions. *Mon. Wea. Rev.,* **110,** 699–706.

Parker, D. E., C. K. Folland, and M. Jackson, 1995: Marine surface temperature: Observed variations and data requirements. *Climatic Change,* **31,** 559–600.

Peng, S., and L. A. Mysak, 1993: A teleconnection study of interannual sea surface temperature fluctuations in the northern North Atlantic and precipitation and runoff over western Siberia. *J. Climate,* **6,** 876–885.

Plaut, G., and R. Vautard, 1994: Spells of low-frequency oscillations and weather regimes in the Northern Hemisphere. *J. Atmos. Sci.,* **51,** 210–236.

Richman, M. B., 1986: Rotation of principal components. *J. Climatol.,* **7,** 13–30.

Robinson, D. A., K. E. Dewey, and R. R. Heim, 1993: Global snow cover monitoring: An update. *Bull. Amer. Meteor. Soc.,* **74,** 1689–1696.

Rogers, J. C., 1984: The association between the North Atlantic oscillation and the Southern Oscillation in the Northern Hemisphere. *Mon. Wea. Rev.,* **112,** 1999–2015.

——, 1997: North Atlantic storm track variability and its association to North Atlantic oscillation and climate variability of northern Europe. *J. Climate,* **10,** 1635–1647.

Serreze, M. C., F. Carse, R. G. Barry, and J. C. Rogers, 1997: Icelandic low cyclone activity: Climatological features, linkages with the NAO, and relationships with recent changes in the Northern Hemisphere circulation. *J. Climate,* **10,** 453–464.

Trenberth, K. E., 1976: Spatial and temporal variations of the Southern Oscillation. *Quart. J. Roy. Meteor. Soc.,* **102,** 639–654.

——, and W.-T. K. Shin, 1984: Quasi-biennial fluctuations in sea level pressures over the Northern Hemisphere. *Mon. Wea. Rev.,* **112,** 761–777.

——, and J. W. Hurrell, 1994: Decadal atmosphere–ocean variations in the Pacific. *Climate Dyn.,* **9,** 303–319.

Vautard, R. P., P. Yiou, and M. Ghil, 1992: Singular-spectrum analysis: A toolkit for short, noisy chaotic signals. *Physica D,* **58,** 95–126.

von Storch, H., and F. W. Zwiers, 1999: *Statistical Analysis in Climate Research* Cambridge University Press, 528 pp.

Wallace, J. M., C. Smith, and Q. Jiang, 1990: Spatial patterns of atmosphere–ocean interactions in the northern winter. *J. Climate,* **3,** 990–998.

Watanabe, M., and T. Nitta, 1998: Relative impacts of snow and sea surface temperature anomalies on an extreme phase in the winter atmospheric circulation. *J. Climate,* **11,** 2837–2857.

Willmott, C. J., C. M. Rowe, and W. D. Philpot, 1985: Small-scale climate maps: A sensitivity analysis of some common assumptions associated with the grid-point interpolation and contouring. *Amer. Cartographer,* **12,** 5–16.

Xie, S.-P., and Y. Tanimoto, 1998: A pan-Atlantic decadal climate oscillation. *Geophys. Res. Lett.,* **25,** 2185–2188.

Yasunari, T., A. Kitoh, and T. Tokioka, 1991: Local and remote responses to excessive snow mass over Eurasia appearing in the northern spring and summer climate. *J. Meteor. Soc. Japan,* **69,** 473–487.

Ye, H., 2000: Decadal variability of Russian winter snow accumulation and its associations with Atlantic sea surface temperature anomalies. *Int. J. Climatol.,* **20,** 1709–1728.

——, 2001: Characteristics of winter precipitation variation over northern central Eurasia and their connections to sea surface temperatures over the Atlantic and Pacific Oceans. *J. Climate,* **14,** 3140–3155.

——, H. Cho, and P. Gustafson, 1998: The changes in Russian winter snow accumulation during 1936–83 and its spatial patterns. *J. Climate,* **11,** 856–863.

Zhang, Y., J. M. Wallace, and D. S. Battisti, 1997: ENSO-like interdecadal variability: 1900–93. *J. Climate,* **10,** 1004–1020.